PROCESSING OF THE NOBEYAMA RADIOHELIOGRAPH DATA

Y. Hanaoka, K. Shibasaki, M. Nishio, S. Enome, H. Nakajima, T. Takano, C. Torii, H. Sekiguchi, T. Bushimata, S. Kawashima, N. Shinohara, Y. Irimajiri [1], H. Koshiishi [2], T. Kosugi, Y. Shiomi, M. Sawa, and K. Kai*

Nobeyama Radio Observatory, National Astronomical Observatory, Minamimaki, Minamisaku, Nagano 384-13, Japan
[1] *Communications Research Laboratory, Koganei, Tokyo, 184, Japan*
[2] *Department of Astronomy, School of Science, University of Tokyo, Bunkyo-ku, Tokyo 113, Japan*

Abstract

The Nobeyama Radioheliograph is a dedicated interferometer to the solar observations, which requires a high time-resolution and a long observational time-coverage. It is important to extract the flare activity during the observing time efficiently from the obtained correlation data. For this purpose, the real-time calibration and imaging are performed with the data processing system of the radioheliograph. The real-time data processing and the CLEAN procedure for the radioheliograph data are described here.

1. Introduction

The Nobeyama Radioheliograph started the regular observation in 1992 June, and some of observational results are presented in these proceedings. This paper is introductory description of the instrumental aspect of the radioheliograph. Since the antennas and the receivers are described in another paper in these proceedings (Nishio et al., 1994), the processing of the radioheliograph data are described here.

The Nobeyama Radioheliograph is a short centimeter-wave (17 GHz) radio-interferometer dedicated to the solar observations. Therefore the data processing has some special features which the other interferometers do not have. The main observational target is solar flares; because of the fast structural changes of flares, a high time-resolution is required for flare observations. Therefore the super-systhesis technique using the earth's rotation cannot be applied to the flare observations. The snap-shot images must have sufficient quality for analyses; it is required that many correlation data from many antennas can be obtained at a time.

* Deseased

Since the flare occurrences can not be predicted, it is required that we take observation time as long as possible to wait for the flare occurrences with a dedicated instrument. However, it is difficult to find when flares occurred and what type of flares occurred during the observations from the recorded data immediately, because the data recorded during the observations are not images but complex correlations. Therefore, images of the sun are synthesized from a part of the correlation data with a high-speed computer and displayed in real-time as quick-look images. We can easily find interesting phenomena from these quick-look images. Although the Nobeyama Radioheliograph is an interferometer, the solar physicists can see the activity of the sun at 17 GHz without being aware of the complexity of the interferometers.

The real-time data storage and processing in the Nobeyama Radioheliograph are described in Section 2, and the CLEAN procedure optimized for the radioheliograph data is described in Section 3.

2. Real Time Data Processing and Storage

The data processing system of the Nobeyama Radioheliograph receives data, stores them, and makes images in real-time; the flow of data are shown in Figure 1. The receiver signals from the 84 antennas of the radioheliograph are processed by the Digital Backend and the raw data sets are produced every 50 msec (these are called as 50-msec data). Each data set consists of 3486(=84C2) complex correlation values for the right- and left-handed circular polarizations and receiver signal amplitudes in RCP and LCP of the 84 antennas. The size of a data set is about 30 KB. Therefore the raw data for an 8-hour observation becomes about 17 GB in size, but this size is too bulky to be stored in a usual data storage. Therefore the raw data are integrated for one second and the produced 1-sec data are transferred to the host computer (NEC SX-JL) and written on optical disks for the permanent recording. The 1-sec data are most basic data in the radioheliograph, and all of them are recorded. The size of the 1-sec data for one day is about 800 MB. The host computer processes a part of the transferred data and displays the images of the sun in real-time. Therefore the host computer must have high performance; it is a mini-super computer which has a computing power of 285 MFlops.

Besides the integration for one second, all of the 50 msec data are recorded by the high-speed digital tape recorder (Sony DIR-1000) temporarily. The 1-sec data are useful for various analyses, but a higher time resolution is required for the analyses of the impulsive behavior of flares. Therefore, flares are searched from the correlation data after the observation, and the 50-msec data of the found flares are played-back from the data tape, transferred to the mini-super computer, and recorded on the optical disks. The data tapes are used for observations again.

These stored data are correlation data, and we can not easily imagine the solar images from the stored data. Therefore quick look images are strongly required for efficient data analyses. In the radioheliograph, a part of the transferred 1-sec data are processed and synthesized to images, and they are displayed and recorded in real time.

The image producing process consists of calibration procedure of antenna phase offsets and gains, inverse Fourier transform to make dirty maps, and CLEAN procedure. The real time calibration is needed to produce images in real time. The self-calibration is done using the data for the image processing. The standard method for the high-quality image restoration for the radioheliograph is described in Section 3, but we use simplified processes for some parts of the real time processing to make maps in short time intervals.

There are three types of the real time image displays. The first one is two-dimensional snapshot maps recorded by a VCR. An example is shown in Figure 2. Such images are displayed every 10 sec, and recorded for 1/3 sec on a video tape. Therefore the solar activity during an eight-hour observation for a day is recorded as a 16-minute video movie. This movie shows the solar activity in a day very comprehensively. The second one is one-dimensional snapshot maps from the correlation data between the antennas in the east-west array. An example is

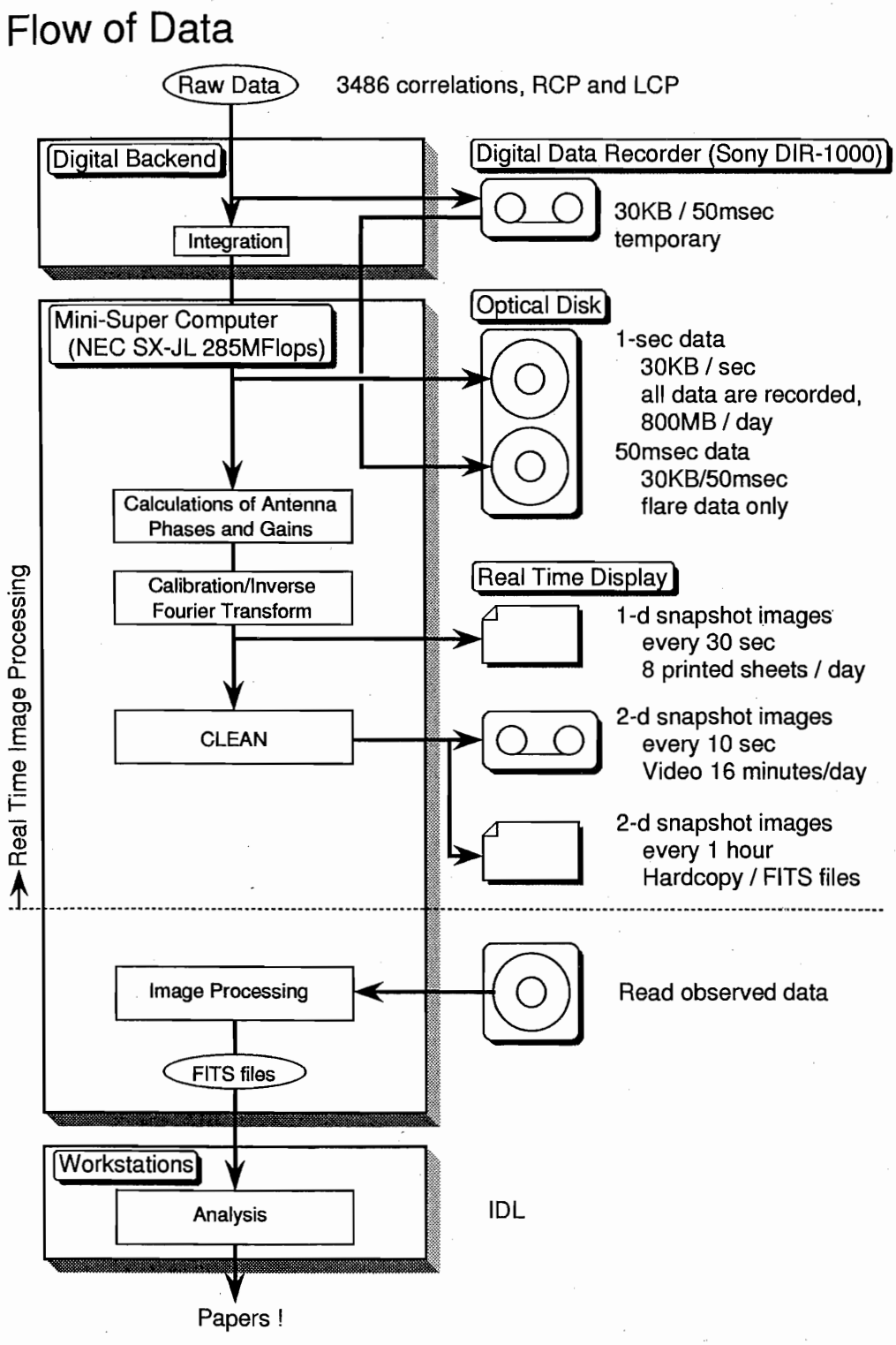

Fig. 1. Data flow diagram of the Nobeyama Radioheliograph.

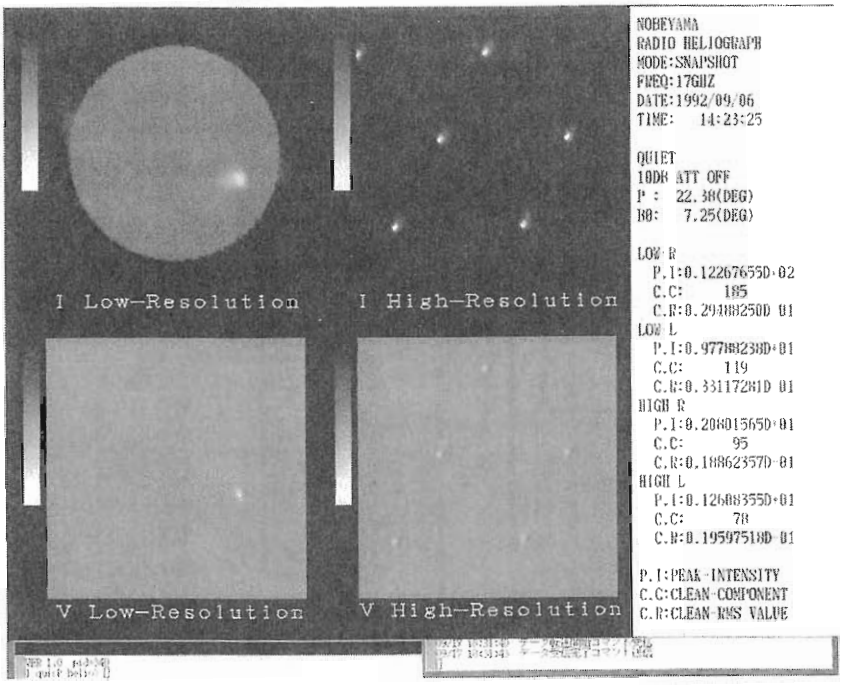

Fig. 2. An example of the real time display of 2-dimensional snap-shot images recorded by a VCR. The upper half shows I (R+L) maps and the lower half shows V (R-L) maps. The left half shows the images of the whole sun made from the Fourier components of the lower spatial frequency. The right half shows the images made from the Fourier components of the higher spatial frequency and they show fine structures; in these images, the various structures are superposed and the images are displayed recursively.

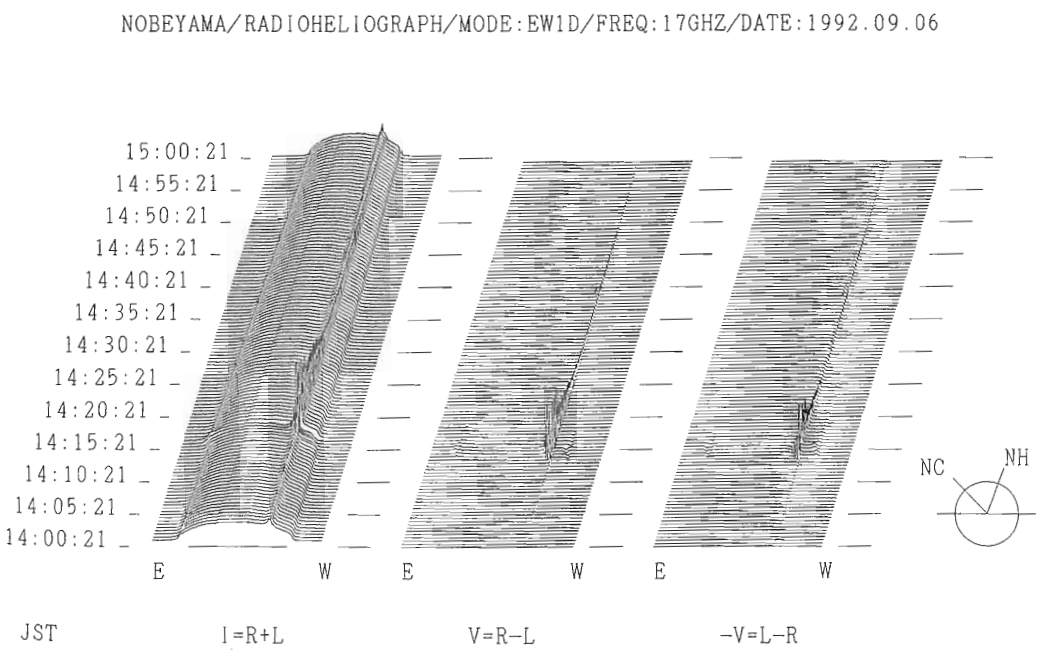

Fig. 3. An example of the real time display of 1-dimensional snap-shot images made from the correlations between the east-west antennas.

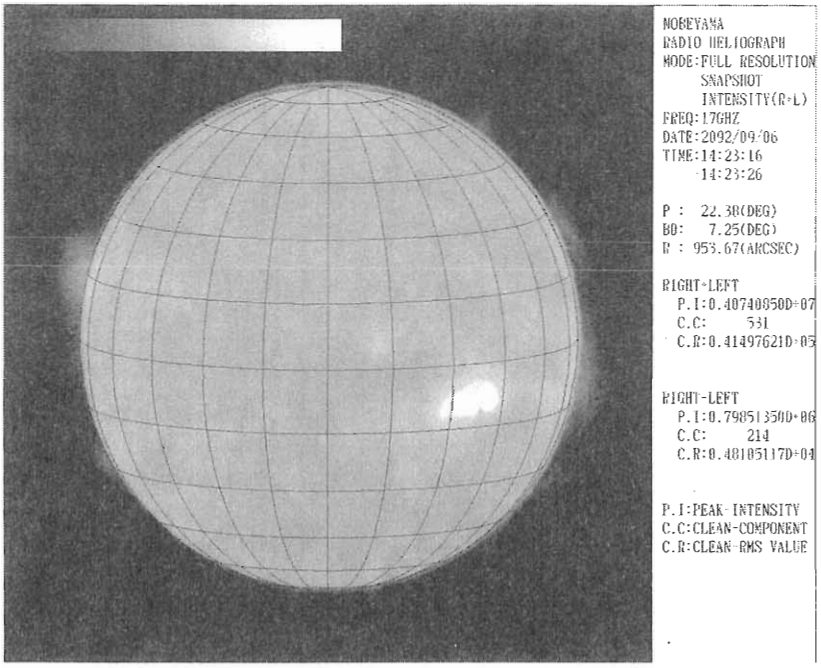

Fig. 4. An example of the real time display of full-resolution 2-dimensional snap-shot images.

shown in Figure 3. A one-dimensional profile is processed every 30 sec, and profiles for one hour are plotted in a sheet. These plots shows time-profiles of flares briefly. The third one is two-dimensional snapshot maps with a high quality. An example is shown in Figure 4. These maps are displayed every one hour.

The above real-time images are only for quick-look; when we decide to analyze an interesting flare found from the quick-look images, we make high-quality images from the recorded correlation data with the method described in Section 3. The host computer is again used to the image processing for the analysis in night time. The processed radio images are analyzed on workstations with the Yohkoh data, optical data, and so on.

3. Image Processing

3.1. Data on the UV-Plane

The array configuration of the antennas is described by Nakajima et al.(1994) and Nishio et al.(1994). The antennas of the radioheliograph are placed at the grid points on a plane with the precision of 0.5 mm. Therefore the correlation data are located at the grid points in the two-dimensional Fourier space (uv-plane) precisely. The uv-coverage map of the snap-shot and the beam of the radioheliograph is shown in Figure 5. The fast Fourier transform (FFT) can be safely applied to such uv data to convert the data in Fourier space into the object space.

An example of a set of observed uv-maps is shown in Figure 6. The inverse-Fourier transformed map from these maps also shown in Figure 6 has no meaning, because each antenna has its own phase offset and gain. The phase offsets and gains of the antennas must be calculated and uv-data must be calibrated before the imaging. Unfortunately the point-sources which are usually used for calibrations of the interferometers are too weak to be detected by the small antennas of the radioheliograph. Furthermore the changes of phases due to atmospheric disturbance are too fast to be calibrated by intermittent observations of point

sources. Therefore we use the sun itself as a calibrator.

The antenna array of the radioheliograph is a redundant array. There are many antenna combinations which have the same spacings in the antennas in the east-west array and those in the north-south array. The correlation values from the antenna combinations which have the same spacing must be the same, but actually they show different values due to antenna phase offsets and gains. Antenna phase offsets and gains are calculated so that the calibrated correlations become the same values.

The number of the redundunt correlations is larger than the number of the antennas. Therefore the phase offsets and the gains are caluculated with the least square method. Since an actual phase difference changes cyclically when the angle of the phase difference increases, the linear least square method can not be applied to calculate the phase offsets. Therefore the phase offsets are calculated iteratively.

Figure 7 shows the calibrated uv-data and the inverse-Fourier transformed image from them. This is a 'dirty' map. This image was taken during a flare, and the image of the sun is much contaminated by the side-lobes of the strong sources. These contaminations are removed by the CLEAN procedure. The disk of the sun is not a circle in Figure 7; its reason is as follows. The element antennas track the sun during the observations, but the interferometer as a whole always points the zenith, and we adopt the uv-plane to be parallel to the ground plane. Therefore the images seen with the interferometer are the projection of the actual objects on the ground plane. The disk of the sun observed with interferometers is generally an ellipse unless the sun is at the zenith. The size of one pixel of dirty maps is 4.649 arcsec square at the zenith.

At first The RCP dirty map and the LCP dirty map are made independently, but the R-L phase difference and gain difference of the receivers are corrected and R+L and R-L dirty maps are created. Generally these dirty maps are cleaned.

3.2. CLEAN procedure

The CLEAN procedure is general method to get original images from incomplete Fourier data of interferometers. The usual CLEAN procedure is useful to remove contaminations of the point-like sources. However, the solar image at 17GHz consists of a disk component and many compact sources. The contribution of the disk component is large except the cases of very intense flares. The efficient CLEAN of the disk component is very important to get images with a high dynamic range. The disk component is not affected by the activity of the sun and it can be replaced a simple model disk. We empirically adopt a flat and circular disk

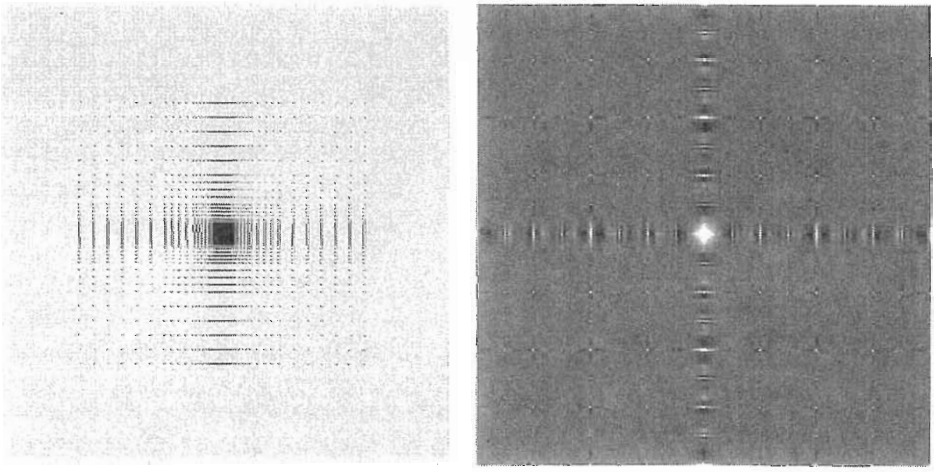

Fig. 5. *left:* The uv-coverage map of the radioheliograph. *right:* The beam of the radioheliograph.

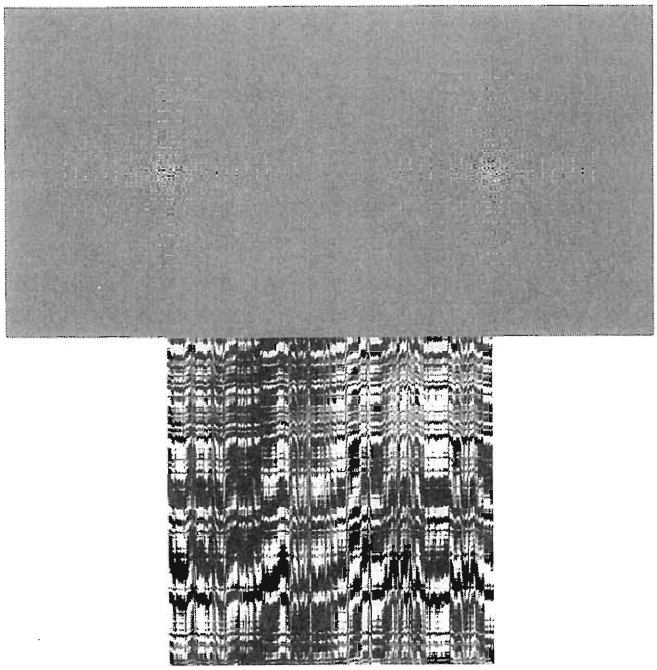

Fig. 6. *top:* Observed uv-maps. The left one is cos component, and the right one is sin component. *bottom:* A dirty map processed from the above uv-maps.

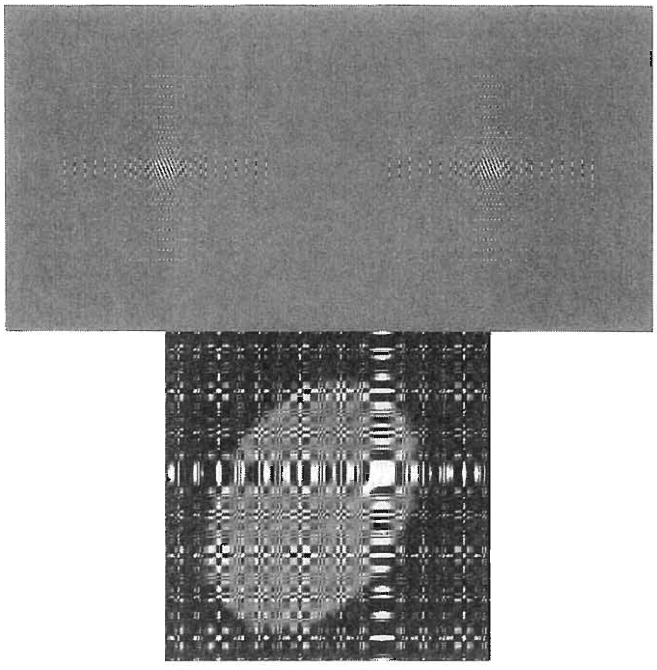

Fig. 7. *top:* Calibrated uv-maps. The left one is cos component, and the right one is sin component. *bottom:* A dirty map processed from the above uv-maps.

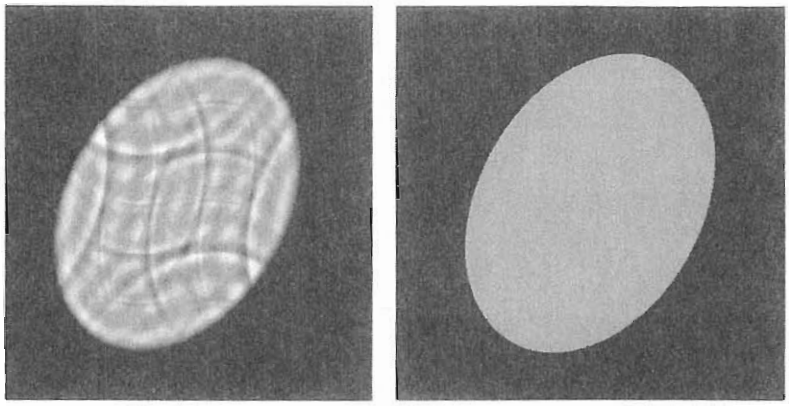

Fig. 8. Model disk *(left)* and a dirty map of the model disk *(right)*.

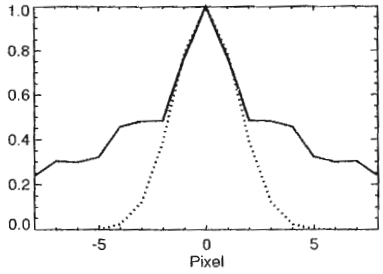

Fig. 9. Comparison between the cross-sectional shape of the dirty beam (solid line) and the clean beam (dotted line). The shape of the clean beam is fitted to the central portion of the dirty beam.

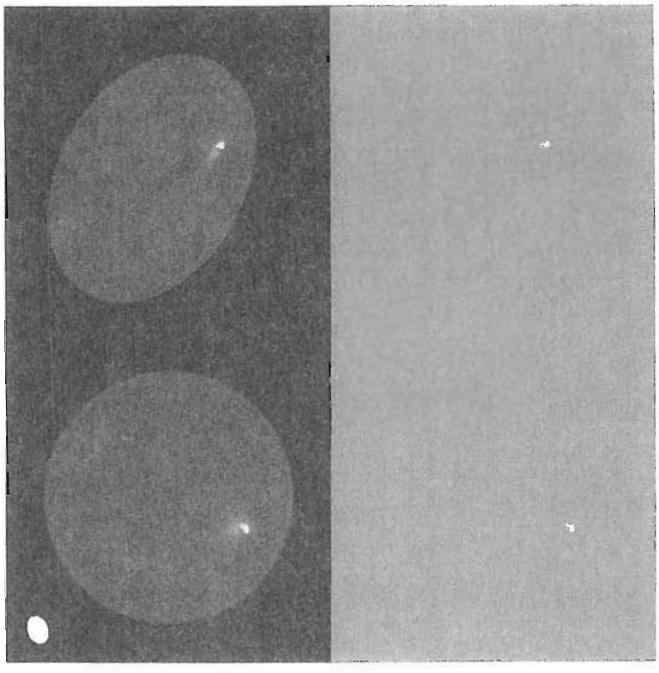

Fig. 10. *top:* Cleaned maps; the left panels show R+L maps, and the right panels show R-L maps. *bottom:* Projection-corrected and beam-corrected cleaned maps. A white patch in the lower-left panel shows the beam shape. Its size is ten times of the actual beam.

whose diameter is 1.25% larger than that of the optical disk as the model disk. An apparent model disk which is calculated from the position of the sun at the observing time of the map in Figures 6 and 7 is shown Figure 8. If the radioheliograph observes it, the dirty map of the model disk becomes the right image of Figure 8.

To cleaning the disk component, the position and brightness of the disk must be estimated accurately. The correlation coefficient between the observed dirty map and the model dirty map, shifting the model step by step. When the correlation coefficient becomes the maximum, the model disk comes the accurate position of the observed sun. The brightness of the disk is calculated from the intensity histogram of the dirty map. The histogram has two peaks; the lower peak corresponds to the brightness of the sky, and the brighter one corresponds to that of the disk. After the determination of the position and brightness of the disk component, the model dirty disk is subtracted from the observed dirty map.

After the subtraction of the model dirty disk, many compact features and diffuse features like active region corona and prominences are left. The compact sources are cleaned then. In the usual CLEAN procedure, the dirty beam is subtracted from the dirty map. However, the compact sources on the sun are rarely point sources; they have dimensions. In our CLEAN procedure the dirty maps of the gaussian sources which have various sizes are used. First, the brightest point in the dirty map are searched. Then, the brightness distribution in the vicinity of the brightest point are compared to those of the dirty maps of the gaussian sources, and the most proper dirty map is subtracted. Such a method contribute to reduce the computing time to make CLEANed maps.

After the subtractions the model disk component and model gaussian source components are restored on the residual image. The dirty beam is substituted by the 'clean beam'. The clean beam is a gaussian source fitted to the central peak of the dirty beam (see Figure 9). The model disk and the model gaussian sources are also convolved with the clean beam before the restoration. The cleaned images of R+L and R-L is shown in the upper panels in Figure 10. These images are transformed to the circular image, where the solar north is to the top and the size of a pixel is 4.91 arcsec square. This image has the same size as a half-resolution SXT image. Finally the beam effect of the element antennas is compensated. Since the FWHM of the beam of the element antennas is about 80 arcmin, the observed brightness at the limb is about 10 % smaller than the actual value; this apparent darkening is corrected. The final results are shown in the lower panels of Figure 10.

The loop gain in our CLEAN procedure is 0.02. If the number of components of the compact sources is 500, the CPU time of the host computer to process a pair of R+L and R-L maps is about three minutes.

References

1. Nakajima, H. et al. 1994, Proc. IEEE, **82**, 705.
2. Nishio, M. et al. 1994, in these proceedings.